

Three-dimensional label-free histological imaging of whole organs by microtomy-assisted autofluorescence tomography

Yan Zhang, Lei Kang, Wentao Yu, Victor Tsz Chun Tsang, Terence T. W. Wong*

Translational and Advanced Bioimaging Laboratory, Department of Chemical and Biological Engineering, The Hong Kong University of Science and Technology, Kowloon, Hong Kong, China

*Corresponding author: ttwong@ust.hk

The Supplementary Material includes:

Supplementary Figure 1 | Experimental characterization of MATE's lateral resolution.

Supplementary Figure 2 | MATE imaging of FFPE thin tissue slices.

Supplementary Figure 3 | MATE imaging of an FFPE mouse brain block.

Supplementary Figure 4 | Imaging depth of MATE in an FFPE mouse brain block.

Supplementary Figure 5 | Calculation of nuclear density map.

Supplementary Figure 6 | Effect of different embedding materials.

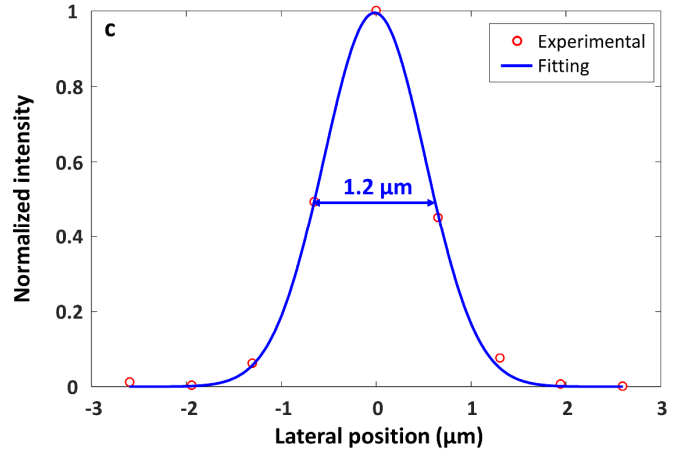
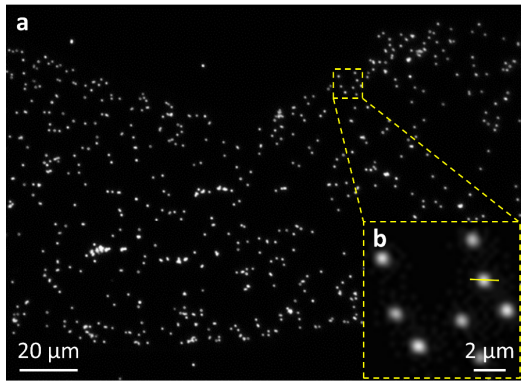
Other Supplementary Material for this manuscript includes the following:

Supplementary Video 1 | Close-up of MATE and H&E-stained images of an FFPE mouse brain block.

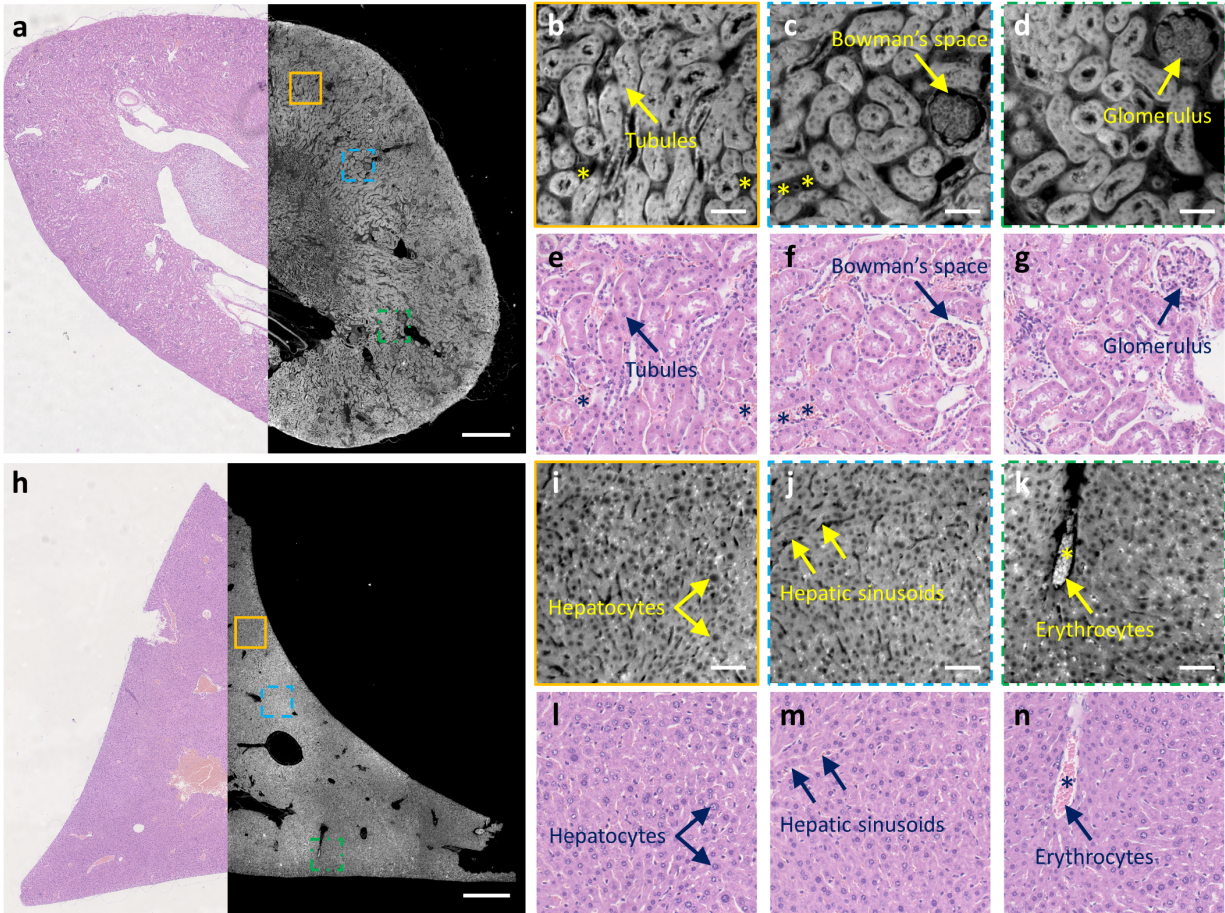
Supplementary Video 2 | A series of coronal sections of an intact FFPE mouse brain imaged by MATE.

Supplementary Video 3 | A series of coronal sections of an FFPE human brain block imaged by MATE.

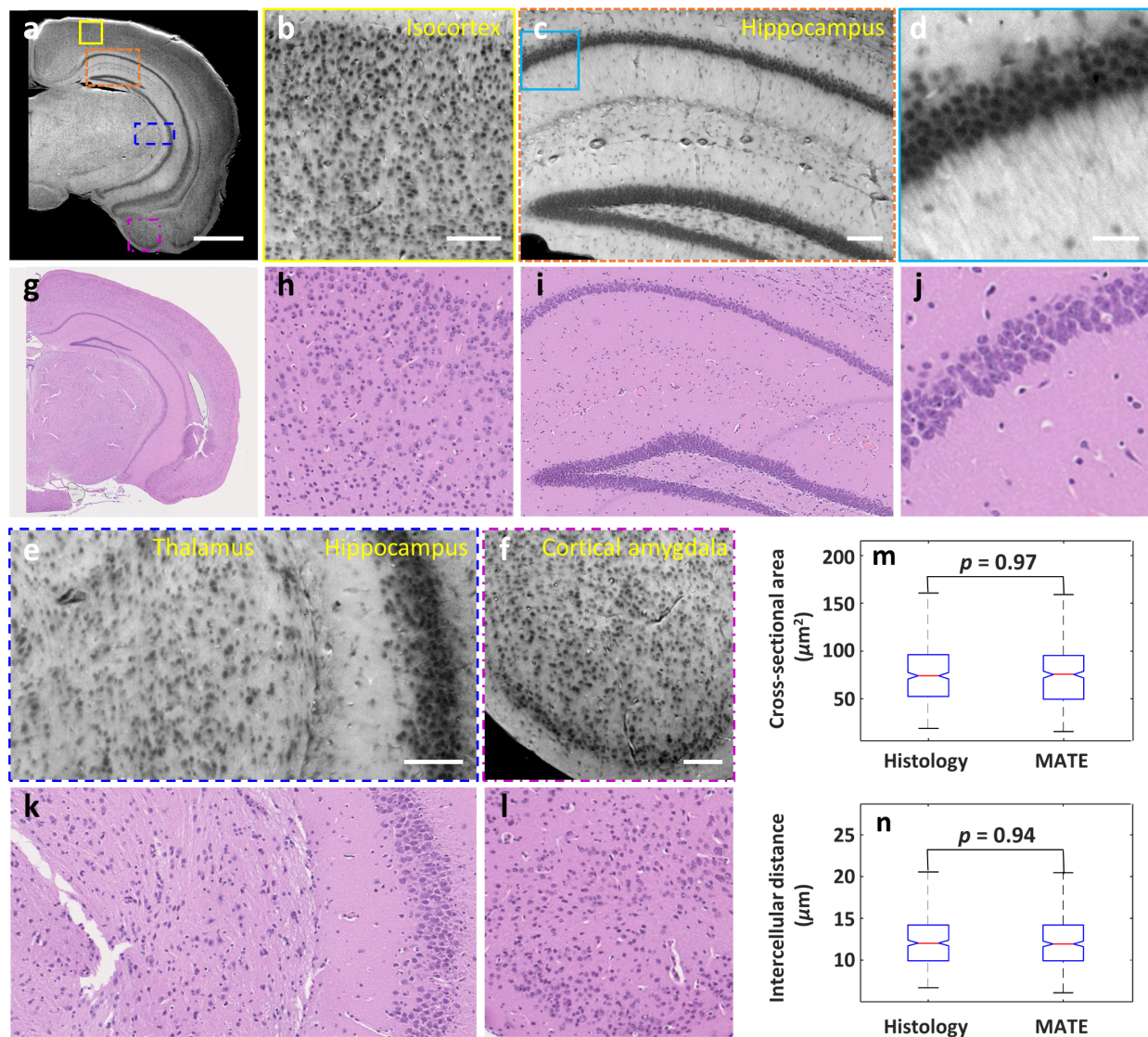
Supplementary Video 4 | High-resolution 3D model of fiber pathways in the white matter of the human brain.



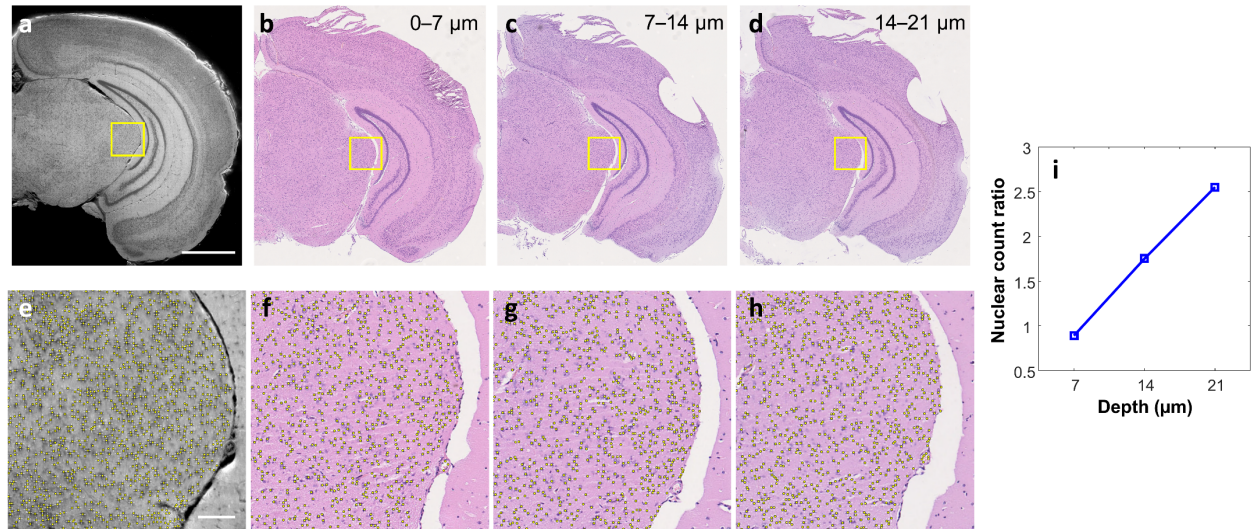
Supplementary Figure 1 | Experimental characterization of MATE's lateral resolution. **a**, A MATE image of blue fluorescent beads (200-nm in diameter with an emission wavelength of 445 nm). **b**, A zoomed-in MATE image of the yellow dashed box in **a**. **c**, Gaussian-fitted intensity distribution along the solid line in **b**, showing that the lateral resolution is $1.2\ \mu\text{m}$.



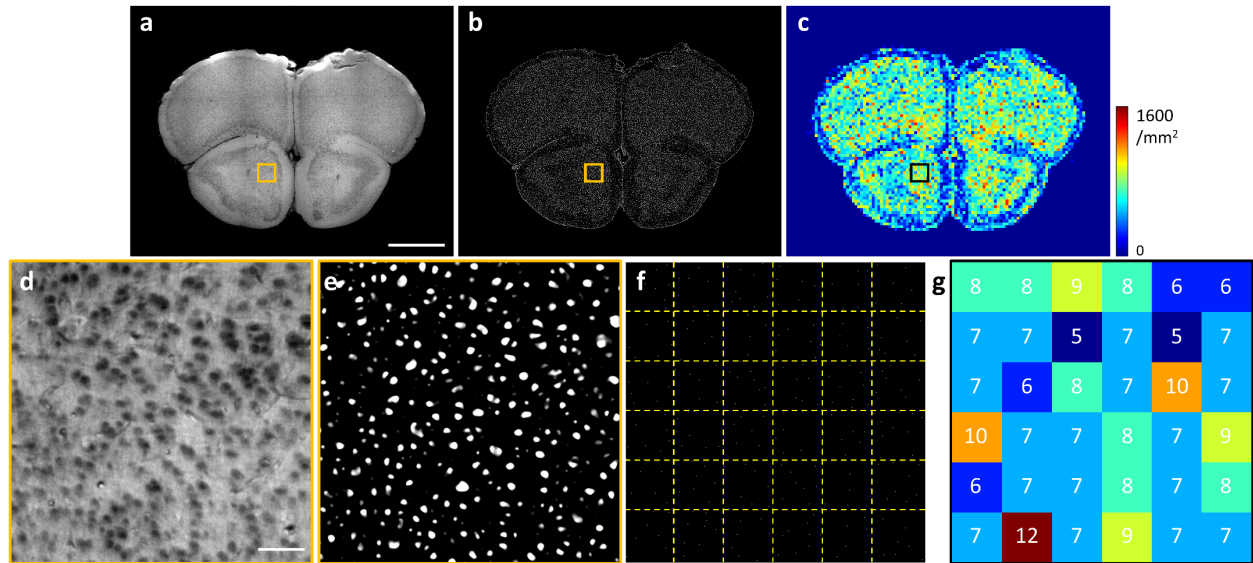
Supplementary Figure 2 | MATE imaging of FFPE thin tissue slices. **a**, A combined MATE and H&E-stained mosaic image of a mouse kidney section. **b–d**, Zoomed-in MATE images of orange solid, blue dashed, and green dashed regions in **a**, respectively. **e–g**, The corresponding H&E-stained images. **h**, A combined MATE and H&E-stained mosaic image of a mouse liver section. **i–k**, Zoomed-in MATE images of orange solid, blue dashed, and green dashed regions in **h**, respectively. **l–n**, The corresponding H&E-stained images. Intensity variations of erythrocytes are denoted by the asterisks. Scale bars, 500 μm (**a**, **h**) and 50 μm (**b–d**, **i–k**).



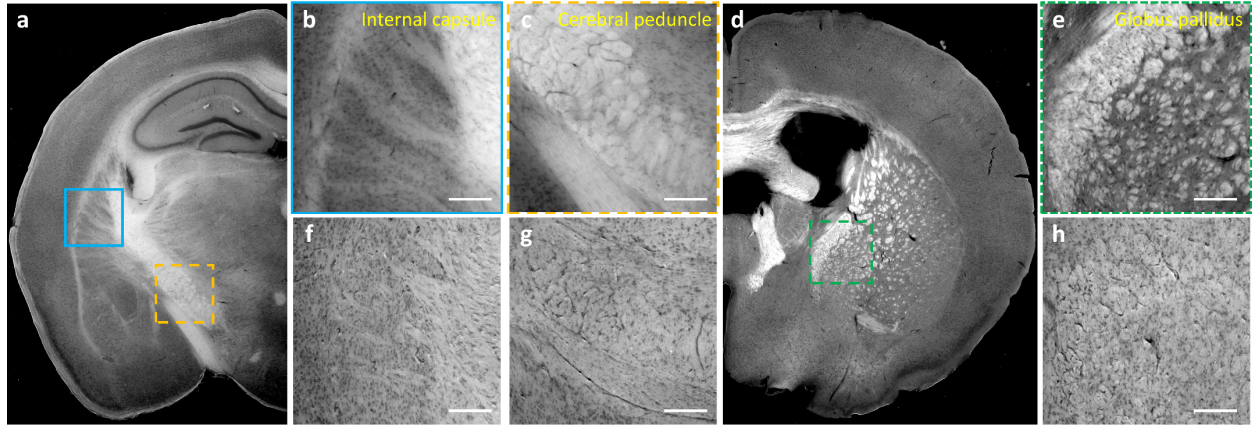
Supplementary Figure 3 | MATE imaging of an FFPE mouse brain block. **a**, A MATE image of an FFPE mouse brain block. **b, c**, Zoomed-in MATE images of yellow solid and orange dashed regions in **a**, respectively. **d**, A zoomed-in MATE image of the blue solid region in **c**. **e, f**, Zoomed-in MATE images of blue dashed and magenta dashed regions in **a**, respectively. **g-l**, The corresponding H&E-stained images. **m, n**, Distributions of cross-sectional area and intercellular distance extracted from **b** and **h**. Scale bars, 1 mm (**a**), 100 μm (**b, c, e, f**), and 30 μm (**d**).



Supplementary Figure 4 | Imaging depth of MATE in an FFPE mouse brain block. **a**, A MATE image of an FFPE mouse brain block. **b–d**, H&E-stained images of thin mouse brain slices which are consecutively sectioned from the block surface with 7-μm thickness. **e–h**, Zoomed-in images of yellow solid regions in **a–d**, respectively. **i**, The ratio of the nuclear count in the H&E-stained images within a given depth range to that in the MATE image. Scale bars, 1 mm (**a**) and 100 μm (**e**).



Supplementary Figure 5 | Calculation of nuclear density map. **a**, A representative MATE image from the mouse brain dataset. **b**, A masked MATE image processed by a Jerman's spherical enhancement filter. **c**, Nuclear density map calculated from **b**. **d,e**, Zoomed-in images of the marked regions in **a** and **b**, respectively. **f**, A binary image that contains center positions of all nuclei in **d**. **g**, A zoomed-in image of the marked region in **c**, with the cell counting performed in every $50\ \mu\text{m} \times 50\ \mu\text{m}$ surrounding area indicated by yellow dashed grids in **f**. Scale bars, 1 mm (**a**) and $50\ \mu\text{m}$ (**d**).



Supplementary Figure 6 | Effect of different embedding materials. **a**, A MATE image of an agarose-embedded mouse brain tissue with 200- μm thickness. **b,c**, Zoomed-in MATE images of the blue solid and orange dashed regions in **a**, respectively. **d**, Another MATE image of an agarose-embedded mouse brain tissue with 200- μm thickness. **e**, A zoomed-in MATE image of the green dashed region in **d**. **f–h**, The corresponding features extracted from a paraffin-embedded mouse brain block. Scale bars, 200 μm .